International Journal of Fluid Machinery and Systems
Vol. 2, No. 3, July-September 2009

**Original Paper**

# A Study of Performance and Internal Flow in a New Type of Sewage Pump

**Yasuyuki Nishi [1] and Junichiro Fukutomi [2]**

[1]ShinMaywa Industries, Ltd.
14 Takumidai, Ono-shi, Hyogo, 675-1322 Japan
[2]Department of Mechanical Engineering, The University of Tokushima
2-1 Minamijosanjima, Tokushima, 770-8506 Japan

**Abstract**

Sewage pumps are designed with a wide flow channel by, for example, sacrificing some efficiency and reducing the number of blades, in order to prevent plugging with foreign bodies. However, the behavior of foreign bodies which actually flow into a pump is extremely complex, and there are questions about whether the presumed foreign bodies will actually pass through. This paper proposes a new type of sewage pump impeller designed to further improve pump efficiency and performance in passing foreign bodies. This sewage pump impeller has a structure in which the suction flow channel of a closed type non-clog pump is wound in a helical spiral. The focus of this research was to investigate pump performance and internal flow in this single blade sewage pump impeller. The results clearly indicated the following facts: The developed sewage pump impeller exhibits high efficiency over a wide range of flow rates; internal flow of the pump is very complicated; and the internal flow state varies greatly when the flow rate changes.

**Keywords**: Turbomachinery, Sewage Pump, Single Blade, Performance, Internal Flow

## 1. Introduction

Sewage pumps used in manhole pump stations and other sewage treatment facilities transport fluids containing large amounts of various solids and fibrous foreign bodies, and thus it is desirable for pumps to have good performance in passing foreign bodies. However, a general technique has not been established for evaluating pump performance in passing foreign bodies, and previously this performance has been evaluated based simply on the size of passed particles relative to the pump diameter (minimum particle size for the flow channel in the pump).

With this background, various types of pumps have been used as sewage pumps in recent years, including: non-clog pumps [1- 4], screw pumps [1, 5] and vortex pumps [1]. These pumps ensure a large passed particle size, while sacrificing some efficiency, by reducing the number of blades or widening the space between the impeller and suction cover. However, the behavior of foreign bodies which actually flow into a pump is extremely complex, and there are questions about whether the presumed foreign bodies can actually pass through. The problem for increasing pump efficiency is that increasing passed particle size causes increased backflow at the blade inlet section and loss in the flow channel, and as a result pump efficiency decreases compared to a multi-blade pump. To address this issue, this paper draws on the characteristics of non-clog impellers and screw impellers, and proposes a new type of pump impeller for sewage [5] in order to further improve pump efficiency and performance in passing foreign bodies.

This sewage pump impeller has a structure in which the suction flow channel of a closed type non-clog impeller is wound in a helical spiral. It is thought that axial flow action based on volume action acts at the axial direction part, and centrifugal action acts at the radial direction part. The pump has the potential to improve pump efficiency and performance in passing foreign bodies because the spiral shaped suction flow channel smoothes the redirection of flow from the axial direction to the radial direction, and causes swirling influx of foreign bodies to avoid the low pressure part at the center of rotation.

Flow in a centrifugal impeller is affected by centrifugal force and Coriolis force, and thus is extremely complex. Numerous studies [6, 7] have previously been done on flow in centrifugal impellers, but almost no research has investigated single blade types like the current impeller. Since a single blade is geometrically asymmetrical, its internal flow is highly unsteady, and is thought to be extremely complex particularly in the case where passed particle size is large, as with the current impeller.

The aim of this research is to elucidate performance and internal flow of the proposed new single blade impeller for sewage pumps. The performance and internal flow are examined by measuring impeller outlet flow using a one-dimensional laser doppler velocimeter,

Received March 12 2009; revised August 18 2009; accepted for publication August 31 2009: Review conducted by Prof. Hyung Hee Cho. (Paper number O09003)
Corresponding author: Yasuyuki Nishi, Dr., nishi.y@sa.shinmaywa.co.jp

and the results are reported.

## 2. Design of new impeller

Since non-clog impellers boost pressure of the working fluid primarily through centrifugal action, a pressure gradient is formed so that there is a balance with centrifugal force in the impeller. Therefore a region of low pressure occurs near the center of rotation, and foreign bodies which has flowed into the impeller may be sucked into that region and cause an obstruction, even if the pump has a large passed particle size. To address this, the authors propose a completely new type of sewage pump impeller which draws on the structure of non-clog impellers (which can easily ensure passed particle size), and screw impellers (which boost pressure of the working fluid through volume action and centrifugal action).

The following basic design conditions were established in order to simultaneously achieve high pump efficiency and good performance in passing foreign bodies:

(1) Ensure a passed particle size the same as the pump diameter.

(2) Use a closed type impeller to prevent engagement of foreign bodies in the blade tip gap.

(3) Shape the suction flow channel into a helical spiral to reduce obstruction by foreign bodies at the low pressure part in the impeller.

(4) Continuously connect the backward inclined single blade to boost pressure of fluid which has passed through the spiral suction flow channel.

As a technique for designing the impeller based on the above basic design conditions, the blade winding angle δ is taken to be a variable, and the spiral suction flow channel is defined by a 3-dimensional curve {f(δ, r(δ), h(δ))} dependent on the radius r(δ) and axial direction length h(δ). The flow channel is formed by the trajectory of a sphere moving along that curve. r(δ) is defined using the following equation so that the angle γ formed with the tangent increases proportionally with δ.

$$r = r_0 \left( \frac{\cos\gamma_0}{\cos\gamma} \right)^C \tag{1}$$

Here the subscript 0 indicates the value when δ=0°, and C is defined by the following equation.

$$C = d\delta / d\gamma \tag{2}$$

On the other hand, h(δ) is defined with the following equation to secure spacing between flow channels in the axial direction so they do not interfere with each other, and to gradually reduce the rate of change as δ increases so that fluid is guided smoothly from the axial direction to the radial direction.

$$h = h_e \left\{ 1 - \left( \frac{\delta}{\delta_e} - 1 \right)^2 \right\} \tag{3}$$

Here, the subscript e indicates the endpoint of the spiral suction flow channel.

Next, a pressure surface is formed by the trajectory of a sphere moving along a curve which does not vary in the axial direction, in order to provide thickness to the negative pressure surface formed by the spiral suction flow channel and make it act as a blade.

The new impeller designed as indicated above tried to improve pump efficiency and performance in passing foreign bodies by smoothing redirection of flow from the axial direction to the radial direction, and causing swirling influx of foreign bodies to avoid the area near the center of rotation.

As a preliminary experiment, a test of passing foreign bodies was conducted by actually introducing into the pump towels and other fibrous foreign bodies which are frequently involved in clogging at facilities such as manhole pump stations. The results confirmed that the new impeller has outstanding performance in passing foreign bodies, with almost no clogging of the impeller compared to conventional non-clog impellers [5].

Fig. 1 shows a basic diagram of the new impeller. The impeller outer diameter is $D_2$=195mm; the blade outlet angle is $\beta_{2b}$=15.1° (pressure side); the winding angle from the blade inlet end to the outlet end is 314°; and the winding angle from the suction inlet to the blade outlet end is 591°. The suction inlet diameter is 114mm; the blade outlet width is $b_2$=80mm; the discharge outlet diameter is 80mm; and the pump has a passed particle size of 80mm from the suction inlet to the discharge outlet.

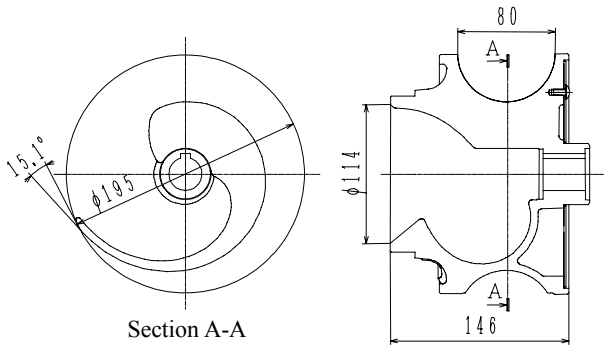


**Fig. 1** New type impeller

## 3. Experimental apparatus and method

### 3.1 Experimental apparatus and method

Fig. 2 shows a schematic diagram of the experimental apparatus. The apparatus is the closed loop type in which liquid flows into the pump from the tank through a suction pipe, passes through a discharge pipe, electro-magnetic water flow meter and gate valve, and returns again to the tank. The experiment was conducted at a rotation speed of n=1740min$^{-1}$. Total head H was determined by measuring pressure on the suction side and discharge side using a strain gauge type compact pressure transducer mounted to the static pressure holes at the front and back of the pump. Flow rate Q was varied using a gate valve mounted to the discharge side, and measured with an electro-magnetic water flow meter. Shaft power L was determined by measuring the rotation speed n with an electro-magnetic pickup, and drive torque T with a torsion bar type torque detector.

### 3.2 Measurement of internal flow

Flow at the impeller outlet was measured using a backscattering one-dimensional laser doppler velocimeter, employing a 200mW argon ion laser as its beam source. With this measurement, it is possible to obtain velocity data only when microparticles have passed measurement points fixed in the space. Therefore, to find the velocity distribution at the impeller outlet it is necessary to find the relative position of the measurement points and the rotating blade. If the apparatus is set to generate a trigger signal each time the impeller rotates, then the time will be 0 every time at that instant. When microparticles pass the measurement points during one rotation, the times $T_1$, $T_2$, ..., $T_N$ from the trigger signal can be obtained. The relative position of the blade and measurement points were found using the times for 1 cycle $T_P$ obtained from this measurement data and the rotation speed.

Fig. 3 shows the velocity measurement points for the impeller outlet. The horizontal direction with respect to the volute casing is defined as the X-axis, and the vertical direction is defined as the Y-axis. Letting $\theta_0$ be the impeller phase angle in the counterclockwise direction from the X-axis, it is assumed that $\theta_0$=0° when the blade outlet end passes the X-axis (i.e. at the position shown in Fig. 3). A total of 7 measurement points are provided at a position 10mm to the outside of the blade outlet end, with a 45° spacing (except at one point) in the counterclockwise direction assuming that θ=0° at the X-axis. For each measurement point, 10,000 measurements were made of $v_u$ and $v_r$, and those were averaged with respect to the impeller phase angle $\theta_0$. About flow rate, the error of measuring instrument oneself is 0.8%. The confidential level of uncertainty is 95%, and the measurement accuracy of this case is about 3 to 4% for velocity.

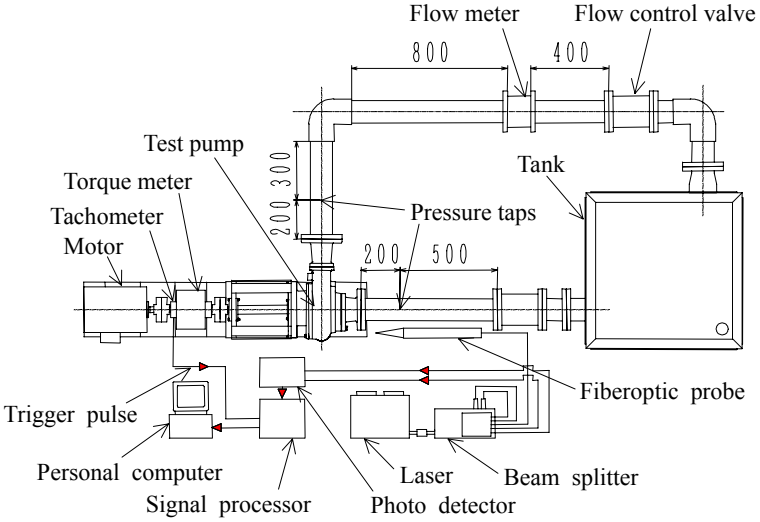


**Fig. 2** Experimental apparatus

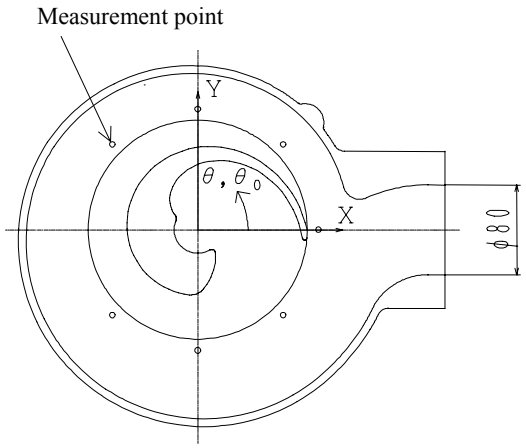


**Fig. 3** Measurement points

## 4. Experiment results and discussion

### 4.1 Performance characteristics

Performance curves are shown in Fig. 4. To ensure that foreign bodies does not cause obstructions in the impeller, the new impeller is designed for a large passed particle size with its single blade. Nevertheless, pump efficiency is a high 67%, which is superior to conventional single blade centrifugal impellers [3, 4]. The reasons for this will have to be examined in more detail in the future, but this impeller is the so-called "bladeless" type, and although its suction inlet is widened somewhat, it has a flow channel with uniform cross-sectional area formed by the trajectory of a sphere to the blade inlet part. Therefore, compared to a conventional single blade centrifugal impeller, there may be less loss due to rapid widening of the blade inlet part, and less impact loss. Reduction in impact loss is thought to be a factor underlying why pump efficiency is high over a wide range of flow rates with the new impeller. Except for near shut-off, the head curve exhibits a downward-sloping linear trend, and does not exhibit upward-sloping unstable characteristics. The shaft power coefficient is low compared to the conventional type, and its curve has limit load characteristics. Therefore it is hard to fall into an overload state even when operated on the high flow rate side. In the best efficiency point, it is Q=0.0225m$^3$/s, H=9.94m, n=1735min$^{-1}$. The specific speed $N_s$(=n(60Q)$^{1/2}$ / H$^{3/4}$) of the pump of this case is 360[min$^{-1}$, m$^3$/min, m], where the dimensionless type number is 0.878.

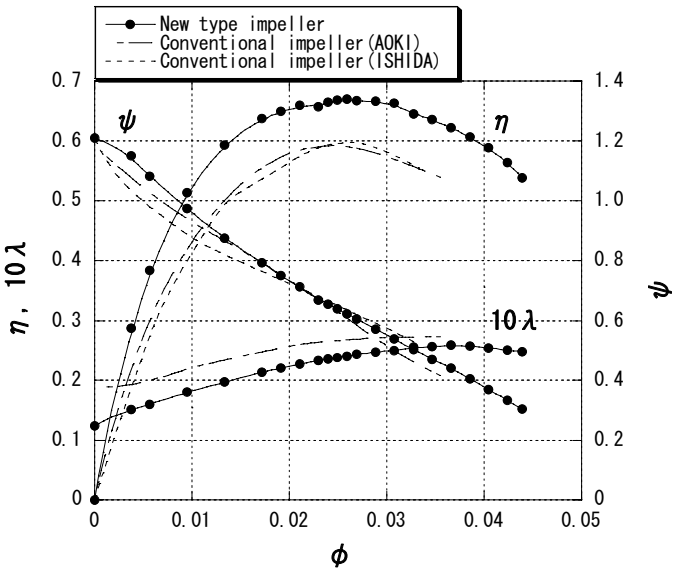


**Fig. 4** Performance curves

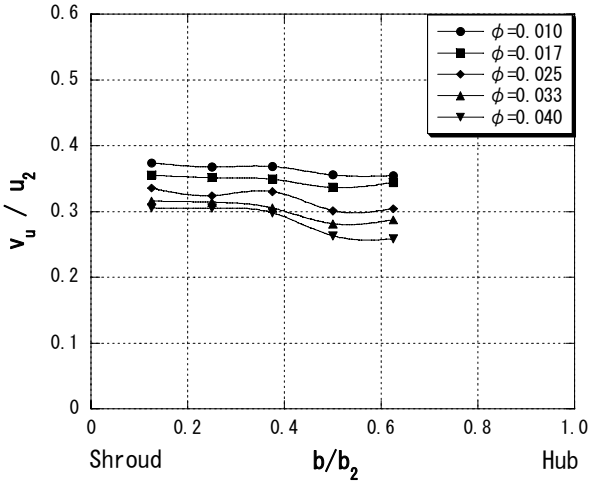


**Fig. 7** $v_u$ distributions in time average（$\theta$ =270°）

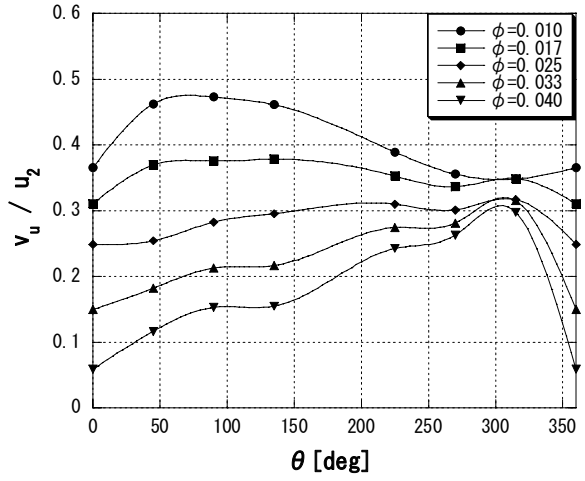


**Fig. 5** $v_u$ distributions in time average（$b/b_2$=0.5）

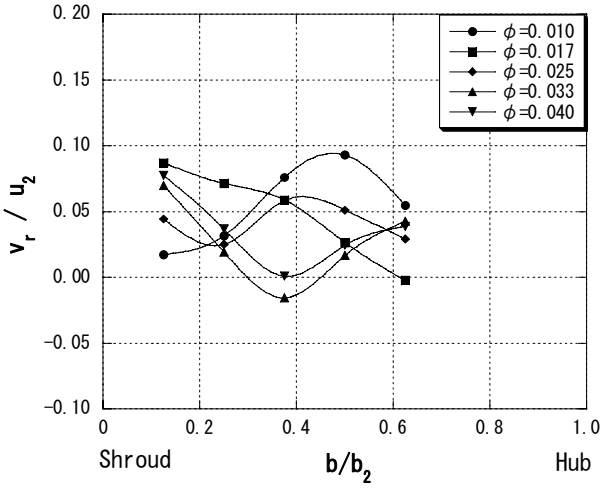


**Fig. 8** $v_r$ distributions in time average（$\theta$ =270°）

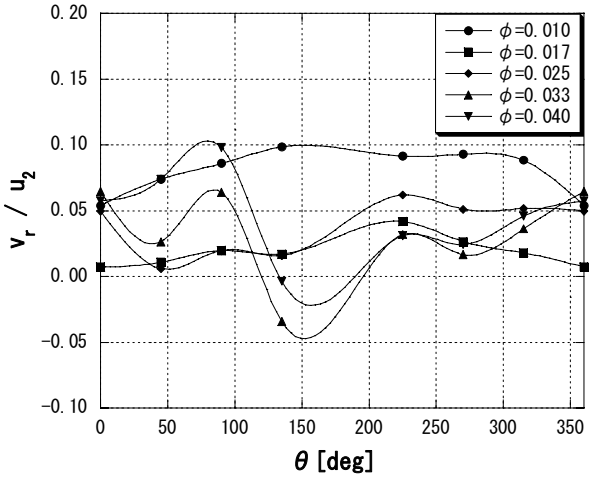


**Fig. 6** $v_r$ distributions in time average（$b/b_2$=0.5）

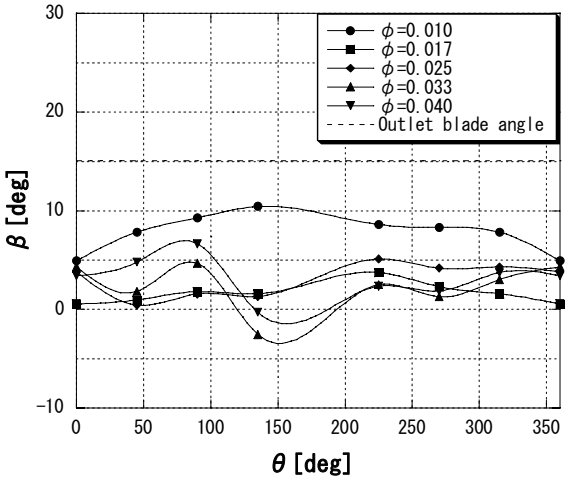


**Fig. 9** $\beta$ distributions in time average（$b/b_2$=0.5）

### 4.2 Time averaged velocity distribution

Fig. 5 and Fig. 6 show, respectively, the circumferential distributions of the circumferential component $v_u$ and radial component $v_r$ of absolute velocity, measured at the width center $b/b_2$=0.5 of the impeller outlet, for each flow rate. Fig. 5 shows that, with a partial flow rate, there is deceleration from the volute winding start to the winding end, and with an excess flow rate,

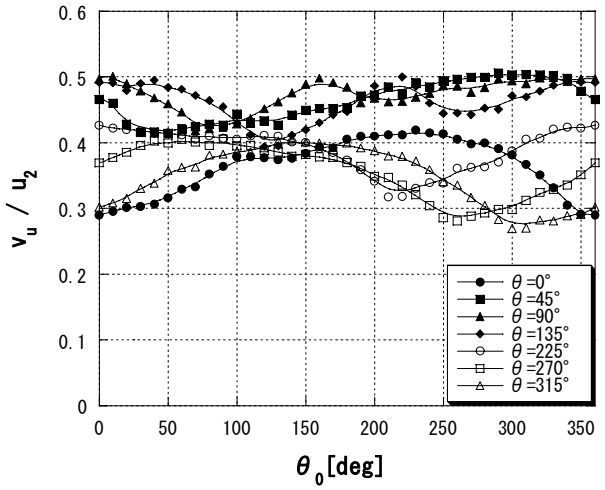


(a) $\phi$ =0.010

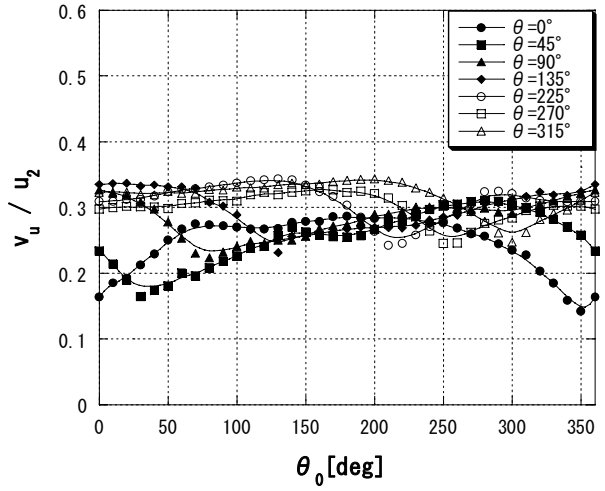


(b) $\phi$ =0.025

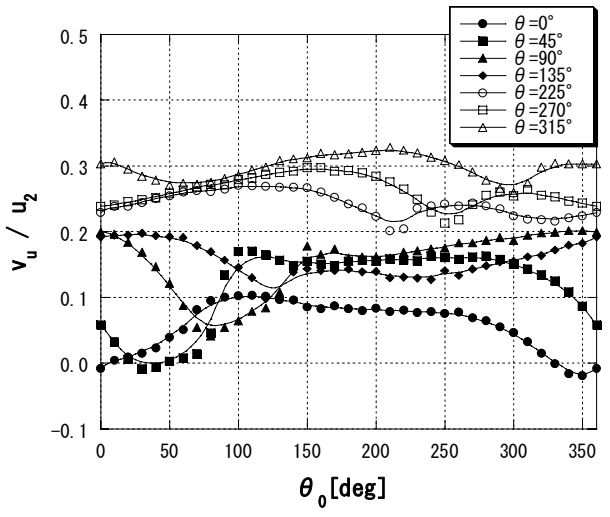


(c) $\phi$ =0.040

**Fig. 10** $v_u$ distributions (b/$b_2$=0.5)

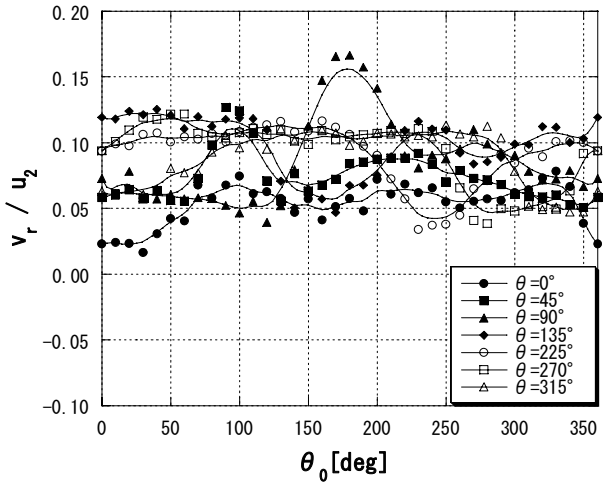


(a) $\phi$ =0.010

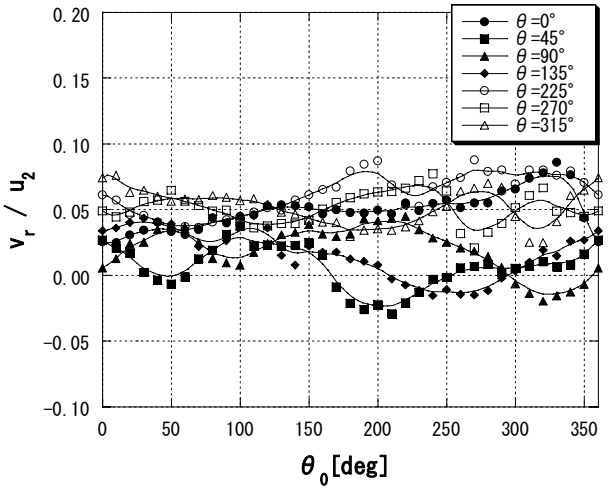


(b) $\phi$ =0.025

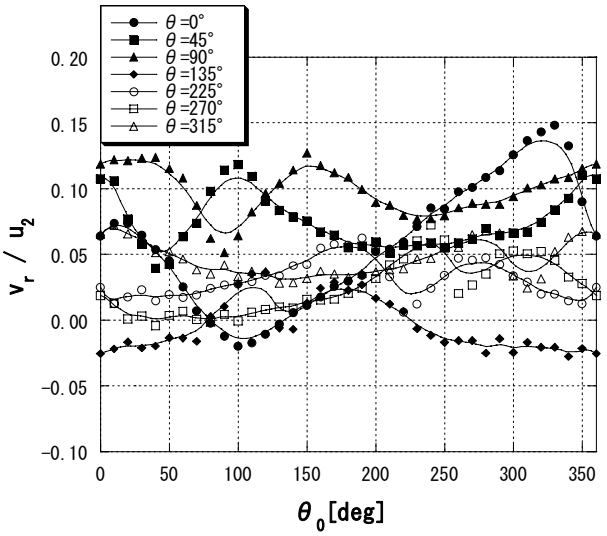


(c) $\phi$ =0.040

**Fig. 11** $v_r$ distributions (b/$b_2$=0.5)

there is acceleration to the winding end. This is the same trend as in experimental results [8] for an ordinary centrifugal impeller.

In Fig. 6, $v_r$ is almost the uniform in the circumferential direction, and has the highest value, for $\phi$ =0.010. In order to satisfy a continuous equation, $v_r$ should exhibit the lowest value with a partial flow rate.

For $\phi$ =0.033 and 0.040, $v_r$ exhibits a negative value near θ=130-190°, and on the other hand, exhibits a relatively high value near θ=40-110° and 220-360°. In terms of time averages, the fluid in the volute flows into the impeller from around θ=130-190°,

and there is formation of a circulating flow which traverses the inside of the impeller and flows out from near the winding start at θ=40-110° and a through-flow which flows out from near θ=220-360° toward the discharge outlet. If the flow rate increases beyond the design flow rate, part of the volute flow will flow into the impeller, which has a wide flow channel, and thus this tendency is likely to be accentuated when there is an excess flow rate.

Fig. 7 and Fig. 8 show, respectively, the width direction distributions of the circumferential component $v_u$ and radial component $v_r$ of absolute velocity, at the measurement point θ=270°, for each flow rate. Fig. 7 shows that $v_u$ increases uniformly as the flow rate becomes partial. In those distributions, $v_u$ is small in the width center and large on the shroud side for all flow rates.

In Fig. 8, $v_r$ is the largest at $b/b_2$=0.5 for $\phi$=0.010, and outflow occurs locally at the width center. It is known that, if 3-dimensional backflow occurs near the wall surface in a centrifugal pump with a specific speed of 220[$min^{-1}$, $m^3$/min, m], then $v_r$ becomes much larger at the width center [9], and the reason why $v_r$ is large at the aforementioned $\phi$=0.010 is due to the effect of the 3-dimensional backflow.

Furthermore, in Fig. 8, $v_r$ exhibits a negative value near $b/b_2$=0.4 for $\phi$=0.033 and 0.040 and then exhibits a higher value toward the shroud side and hub side. This shows that the aforementioned through-flow flows out at a high rate from the shroud side or hub side.

Fig. 9 shows circumferential distributions of the relative flow angle β at the width center $b/b_2$=0.5 of the impeller outlet for each flow rate. In Fig. 9, the relative flow angle β is quite small with respect to the blade outlet angle $\beta_{2b}$=15.1° for all flow rates except $\phi$=0.010. It is evident that, because this impeller is single blade, it is greatly affected by slip.

From the above it can be seen that the internal flow of this pump is extremely complex, and the internal flow state varies greatly in the circumferential and width direction as the flow rate changes.

### 4.3 Velocity distributions during a single impeller rotation

Figs. 10 (a)-(c) and Figs. 11 (a)-(c) show, respectively, the velocity distributions for the circumferential component $v_u$ and radial component $v_r$ of absolute velocity at the width center $b/b_2$=0.5 during a single impeller rotation for each flow rate. Figs. 10 (a)-(c) show that there is an overall decrease in $v_u$ at each measurement point as the flow rate moves to excess, regardless of $\theta_0$. With $\phi$=0.025, $v_u$ is uniform regardless of $\theta_0$ at θ=90-315° near the winding end. However, at the measurement points θ=0° and 45°, $v_u$ is lowest when $\theta_0$=350° and 30°, respectively. With $\phi$=0.040, that tendency is even more conspicuous; $v_u$ exhibits a value close to 0, and this may be the branch point between the aforementioned circulating flow and through-flow.

In Figs. 11(a)-(c), $v_r$ exhibits high values overall to the degree that the flow rate moves to excess, regardless of $\theta_0$, except at $\phi$=0.010 where there is a local outflow at the width center. However, just as $v_r$ exhibited negative values near θ=130-190° in Fig. 6, at the measurement point θ=135° the region where $v_r$ becomes negative is larger for $\phi$=0.040 than for $\phi$=0.025. Examining $\phi$=0.040 more closely, $v_r$ exhibits a negative value at the measurement point θ=135° when $\theta_0$=0-80° and 230-360°, and $v_r$ is high overall for the measurement points θ=0-90°and 270-360° on the +X-axis side, particularly when $\theta_0$=230-360° near the winding end. That is, when fluid is discharged at a high rate near the discharge outlet and winding start, with the tip of the blade pressure side near the winding end, fluid is conversely sucked into the impeller near θ=135° on the opposite side.

For $\phi$=0.010, $v_r$ exhibits its maximum value when $\theta_0$=80-110° at the measurement point θ=45°, and when $\theta_0$ = 160-200° at the measurement point θ=90°. This may be due to the fact that recirculating flow increases and has a large impact on the blade outlet flow, particularly when there is a partial flow rate, because the flow channel near θ=45° and 90° abruptly enlarges due to the blade position when the blade outlet end passes the tongue section.

Also, in all the graphs, both $v_u$ and $v_r$ decrease at almost the back end position of the blade outlet. The following will discuss the reason for this based on the distributions of relative velocity w and relative flow angle β at the width center during a single impeller rotation at $\phi$=0.025 shown in Fig. 12 and Fig. 13. In Fig. 12, for each measurement point w there is an abrupt increase and decrease before and after passing the blade outlet end, and then a decrease. Therefore, the flow between blades is somewhat fast on the suction side, and exhibits a velocity distribution close to slow inviscid flow on the pressure side. Looking also at Fig. 13, as the blade outlet end approaches each measurement point, w increases with the decrease in β and after passing, w decreases

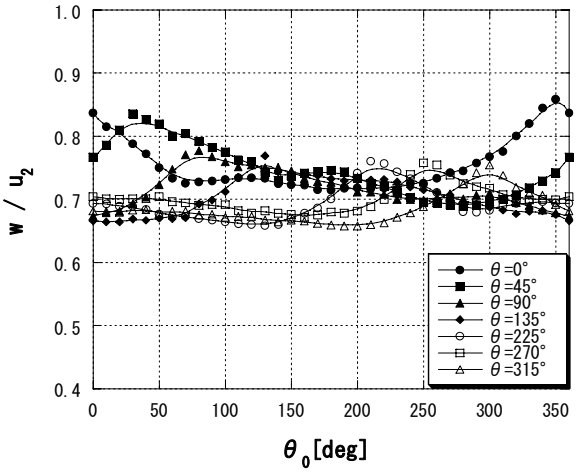


**Fig. 12** w distributions ( $\phi$=0.025, $b/b_2$=0.5)

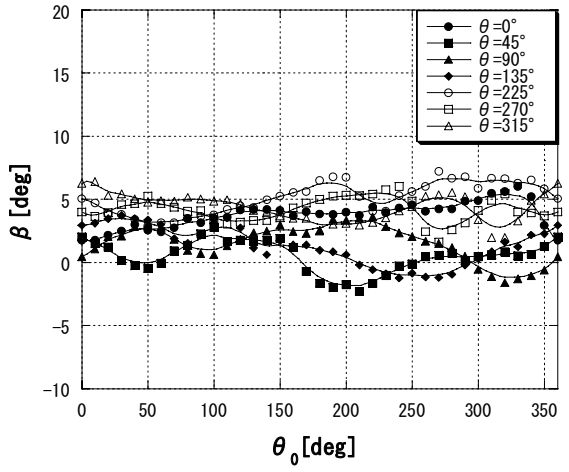


**Fig. 13** β distributions ( $\phi$=0.025, $b/b_2$=0.5)

with the increase in β. Due to the above, the aforementioned decrease in $v_u$ and $v_r$ is thought to be due to an increase in w caused by the fact that fluid flows along the trailing edge where the blade angle is small, and the fact that a flow from the blade pressure side toward the suction side is induced at the blade outlet.

**4.4 Slip factor**

This section examines the slip factor of this impeller, which is a single blade. The slip factor is defined by the following equation.

$$k = \frac{v_{u2\infty} - v_{u2}}{u_2} \tag{4}$$

Here the subscript $\infty$ is for the case with no slip. Therefore, k can be determined by measuring $v_{u2}$ for the impeller outlet.

There is also another method of finding k, from the shaft power. If it is assumed that there is no prewhirl at the blade inlet, then $v_{u2}$ is given by the following equation.

$$v_{u2} = \frac{gH_{th}}{u_2} \tag{5}$$

Here the subscript th is a theoretical value, and the shaft power L is given by the following formula.

$$L = L_{th} + L_l + L_{df} + L_m \tag{6}$$

Here $L_{df}$ is disk friction loss, $L_l$ is leakage loss and $L_m$ is mechanical friction loss. Thus, $H_{th}$ is given by the following equation.

$$H_{th} = \frac{L - L_{df} - T_0\omega}{\rho g(Q+q)} \tag{7}$$

Here $T_0$ is empty rotation torque, q is the leakage flow rate, and ω is the rotation angular speed. The disk friction loss $L_{df}$ is estimated using the following equation [10].

$$L_{df} = C_d \rho u_d^3 D_d^2 \tag{8}$$

Here, $C_d$ is the disk frictional resistance coefficient, $D_d$ is the disk diameter, and $u_d$ is the velocity of the disk circumference. The actual measurement is used for empty rotation torque $T_0$, and the leakage flow rate q is estimated by applying the following equation [11] to the annular gap part, and using the actual measurement for pressure.

$$q = \kappa\sqrt{2g\Delta h}\pi d_r b \tag{9}$$

$$\kappa = \frac{1}{\sqrt{(\lambda_w l / 2b_r) + 1.5}} \tag{10}$$

Here, $b_r$ is the gap width, $d_r$ is the average diameter of the annular gap part, Δh is the static pressure head difference before and after the gap, l is the length of the gap part, and $\lambda_w$ is the friction coefficient. The slip factor k is calculated from Equation (4) using the above equations.

The slip factor is also found using the following Wiesner formula [12]. First, ε is given by the following equation.

$$\varepsilon = \frac{1}{\exp(\frac{8.16\sin\beta_2}{z})} \tag{11}$$

In this impeller, $r_1 / r_2 > \varepsilon$ holds, and thus the slip factor k is given by the following equation.

$$k = 1 - (1 - \frac{\sqrt{\sin\beta_2}}{z^{0.7}})\left\{1 - \left(\frac{r_1}{r_2} - \varepsilon\right)^3 / (1-\varepsilon)^3\right\} \tag{12}$$

Here, z is the number of blades. Using the above, the slip factor k is calculated by substituting specifications in Equation (12).

Fig. 14 shows a comparison of the slip factor found from the flow field and shaft power, and the value found from the Wiesner formula. However, the slip factor found from the flow field is determined by using flow at the width center $b/b_2$=0.5 as a typical value, and correcting velocity measured immediately after the impeller outlet to the impeller outlet value. When these values are

compared, they almost match near the best efficiency point, and the value is quite large with k=0.53. Also, the values found from the flow field and shaft power follow the values found from the Wiesner formula over a wide range of flow rates.

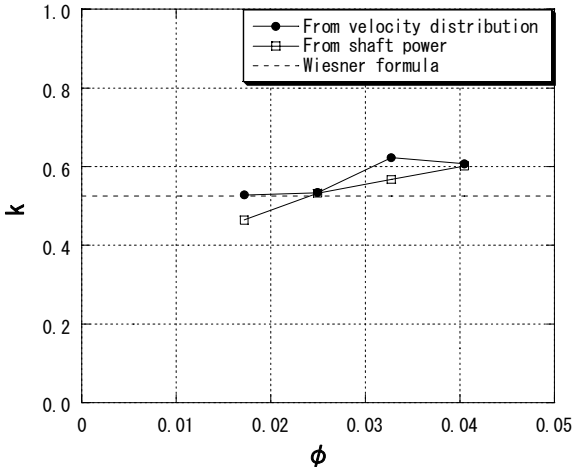


**Fig. 14** Slip factor

## 5. Conclusion

The authors proposed a new type of pump impeller for sewage, and experimentally investigated its performance and internal flow. The following points became clear as a result.

(1) Even though a large passed particle size is achieved with a single blade, the impeller has high efficiency, and the range exhibiting high efficiency is broad.

(2) At partial flow rates, the radial component of absolute velocity is largest in the width center, and there is a local outflow.

(3) At excess flow rates, there is a circulating flow in which part of the volute flow traverses the inside of the impeller and flows out from near the winding start, and a through-flow which flows out from near the winding end.

(4) The internal flow state varies greatly in the circumferential and width direction as the flow rate varies.

(5) When fluid is discharged at a high rate near the discharge outlet and winding start, with the tip of the blade pressure side near the winding end, fluid is conversely sucked into the impeller on the opposite side.

(6) Since this impeller is a single blade, the effects of slip are large. The slip factor found from the flow field at the width center and the shaft power almost matches the value found from the Wiesner formula near the best efficiency point.

## Nomenclature

| | |
|---|---|
| $b_2$ | Blade outlet width [m] |
| $D_2$ | Impeller outer diameter [m] |
| $g$ | Gravitational acceleration [m/s$^2$] |
| $H$ | Total head [m] |
| $L$ | Shaft power [W] |
| $n$ | Rotation speed [mim$^{-1}$] |
| $Q$ | Flow rate [m$^3$/s] |
| $u$ | Tangential velocity [m/s] |
| $v$ | Absolute velocity [m/s] |
| $w$ | Relative velocity [m/s] |
| $\beta$ | Relative flow angle [° ] |
| $\eta$ | Pump efficiency (= $\rho gQH/L$) |
| $\lambda$ | Shaft power coefficient (=$L/(\rho \pi D_2 b_2 u_2^3/2)$) |
| $\phi$ | Flow rate coefficient (=$Q/(\pi D_2 b_2 u_2)$) |
| $\psi$ | Head coefficient (=$H/(u_2^2/2g)$) |
| $\theta$ | Circumferential position [° ] |
| $\theta_0$ | Impeller phase angle [° ] |
| $\rho$ | Fluid Density [kg/m$^3$] |

*subscript*

| | |
|---|---|
| *1* | Blade inlet |
| *2* | Blade outlet |
| *r* | Radial component |
| *u* | Circumferential component |

## References


[1] Hiraoka, M. et al, 1997, ‘‘Japan institute of Wastewater Engineering Technology, Wastewater Manhole Pump Technology Manual-June 1997,’’ p. 18. (in Japanese).

[2] Okamura, T., 1979, ‘‘Radial Thrust in Centrifugal Pumps with Single Vane Impeller,’’ Transactions of the Japan Society of Mechanical Engineers, Series B, Vol. 45, No. 398, p. 1458. (in Japanese).

[3] Aoki, M., 1984, ‘‘Instantaneous Pressure Distribution between Blades and Fluctuating Radial Thrust in the Single Blade Centrifugal Pump,’’ Transactions of the Japan Society of Mechanical Engineers, Series B, Vol. 50, No. 451, p. 661. (in Japanese).

[4] Ishida, I., 2002, ‘‘The Consideration in the Radial Thrust Decrease of Centrifugal Pump,’’ Turbomachinery, Vol. 30, No. 12, p. 741. (in Japanese).

[5] Nishi, Y. et al, 2005, ‘‘Development of Submersible Pump Having High Efficiency and High Passage Performance,’’ ShinMaywa Technical report, No. 27, p. 8. (in Japanese).
[6] Johnson, M.W. and Moore, J., 1983, ‘‘Secondary Flow Mixing Losses in a Centrifugal Impeller,’’ Transactions of the American Society of Mechanical Engineers, Journal of Engineering for Power, Vol. 105, No. 1, p. 24.
[7] Eckardt, D., 1976, ‘‘Detailed Flow Investigations within a High-speed Centrifugal Compressor Impeller,’’ Transactions of the American Society of Mechanical Engineers, Journal of Fluids Engineering, Vol. 98, No. 3, p. 390.
[8] Kurokawa, J. et al, 1983, ‘‘Theoretical and Experimental Determinations of the Flow Characteristics in Volute (2nd Report, Experimental Results for Two-Dimensional Log-Spiral),’’ Transactions of the Japan Society of Mechanical Engineers, Series B, Vol. 49, No. 448, p. 2735. (in Japanese).
[9] Kurokawa, J. et al, 1984, ‘‘Prediction of Outlet Flow Characteristics of Centrifugal Impellers (1st Report, Consideration of Velocity Distribution),’’ Transactions of the Japan Society of Mechanical Engineers, Series B, Vol. 50, No. 459, p. 2777. (in Japanese).
[10] Toyokura, T. and Kita, C., 1986, ‘‘Volute Pump Fundamentals and Design Drawings,’’ p.32, Jikkyo Shuppan. (in Japanese).
[11] Takagi, T., 1964, ‘‘Causes of Difference Between the Performances of Actual Francis Water Turbines and Their Models,’’ Transactions of the Japan Society of Mechanical Engineers, Vol. 67, No. 544, p. 671. (in Japanese).
[12] Wiesner, F. J., 1967, ‘‘A Review of Slip Factors for Centrifugal Impellers,’’ Transactions of the American Society of Mechanical Engineers, Series A, Vol. 89, No. 4, p.559.